Analysis of Minor Components by Ultrahigh Resolution NMR. 2. Detection of 0.01% Diacetone Alcohol in "Pure" Acetone and Direct Measurement of the Rate of the Aldol Condensation of Acetone

Steven R. Maple and Adam Allerhand*

Contribution from the Department of Chemistry, Indiana University, Bloomington, Indiana 47405. *Received January 26, 1987*

Abstract: Ultrahigh resolution NMR methodology permits the detection of as little as 0.01% $CH_3COCH_2(OH)C(CH_3)_2$ (**2**) in a sample of "pure" acetone (**1**) of natural isotopic composition, with the use of the methyl resonances in the proton-decoupled ^{13}C NMR spectrum, even though the resonances of **2** are very close to those of **1**. Also, all three peaks of the triplet of the $^{13}CH_2D$ carbon of $^{13}CH_2D$–^{12}CO–$^{12}CH_3$ are fully resolved, even though their intensity is only 0.015% of that of the main contributor to the spectrum, $^{13}CH_3$–^{12}CO–$^{12}CH_3$, and one of the peaks of the triplet is only 7 Hz away from the main acetone peak. The intensities of the $^{13}CH_2D$ triplet serve as a calibrator of dynamic range accuracy in ^{13}C NMR measurements of relative proportions of major and minor components. After addition of aqueous sodium hydroxide to the acetone sample, the growth of the methyl carbon resonances of **2** provides a direct measurement of the rate constant for the aldol dimerization of **1** and also the equilibrium constant for this reaction. This example demonstrates the ability of ultrahigh resolution NMR to study directly the kinetics of reactions that have equilibria highly displaced toward the reagents, instead of the traditional procedure of monitoring only the kinetics of the reverse reaction by starting with pure "products". Artifacts that may interfere with the study of minor components by ultrahigh resolution NMR are discussed.

This report deals with applications of NMR spectroscopy for studying minor components in mixtures *without* prior separation from major components by chromatography or other methods. Here we define a minor component as one whose molar concentration is 0.1% or less of that of a major one. We are particularly interested in the nonseparative detection and identification of minor components whose chemical shifts are very similar to those of major ones. Until recently, such a task required the suppression of the resonances of the major components by means of methods that selectively diminish the amplitude of some resonances. The classic and most exhaustively used example of such suppression has been the "elimination" of the H_2O signal in ^1H NMR studies of biologically important molecules dissolved in H_2O instead of D_2O, such as studies of exchangeable hydrogens and intact cells.[1-7] However, peak suppression may be difficult or undesirable when there are many major resonances, when one or more of the small resonances is very close to a major one, or when it is important to measure the relative proportions of the major and minor components. Recently we have shown that ultrahigh resolution methodology[8-12] enables the NMR spectroscopist to study minor components without suppression of the resonances of the major ones,[13,14] even when each minor resonance has only 10^{-4} the intensity of a major one and when the separation between the major and minor peaks is 100 Hz or even less.[14]

In this paper we apply ultrahigh resolution NMR methodology to show that reagent grade acetone (**1**) contains small amounts of 4-hydroxy-4-methyl-2-pentanone (**2**), commonly called "diacetone alcohol", which is the aldol condensation dimer of **1**. We then show that the rate of formation of **2** can be monitored directly, even though the equilibrium is highly displaced toward **1**. In the past, only the kinetics of the decomposition of **2** into **1** has been measured directly.

We also present data about various experimental difficulties that may arise in studies of minor components by ultrahigh resolution NMR spectroscopy.

Experimental Section

Materials. Analytical reagent grade acetone from Mallinckrodt and "spectranalyzed" acetone from Fisher were used for minor component detection. The sample for the aldol condensation study contained Fisher "spectranalyzed" acetone. Diacetone alcohol (98% purity) and cyclohexane-d_{12} were obtained from Aldrich Chemical Co. and Cambridge Isotope Laboratories, respectively.

Instrumentation. Proton-decoupled ^{13}C NMR spectra were recorded at 50.31 MHz and 26.5 °C, on a Nicolet NT-200 spectrometer, modified as described.[8-12] It was equipped with a 10-mm bottom-loading probe from Cryomagnet Systems, Inc.[12] Standard 10-mm tubes (513-7PP from Wilmad Glass Co.) were used with about 3-mL sample volume. The spinner speed was modulated, in the range from about 10 to about 20 Hz, in order to smear out spinning sidebands.[15]

Detection of Minor Components. The spectrum of **1** from Mallinckrodt (with 20% v/v cyclohexane-d_{12}) shown in Figure 1 was recorded with the use of 90° radio frequency pulse excitation, a spectral width of ±300.12 Hz (quadrature detection), 64K time-domain points, an acquisition time of 54.59 s per scan, and 6000 scans. The accumulation and processing conditions described below were designed to take into account the limitations imposed by the 12-bit analog-to-digital converter (ADC) and 20-bit word of our Nicolet-1280 computer. The 12-bit ADC was marginally adequate, because the single-scan signal-to-noise ratio of the main methyl carbon resonance was about 2000. We used double precision (40-bit word), as described below, to obtain the 6000-scan spectrum of Figure 1, where the main resonance has a signal-to-noise ratio of about 130000. The 6000 scans were the final result of 300 batches of 20 scans each. Specifically, 380 single-precision (20-bit word) 20-scan time-domain batches were acquired; homogeneity adjustment (Z_1 gradient only) was automatically implemented prior to each 20-scan batch under software control; the 300 batches with the narrowest line widths were consolidated into 30 single-precision 200-scan time-domain spectra, each of which was subjected to 30 mHz Lorentzian broadening

(1) Redfield, A. G.; Gupta, R. K. *J. Chem. Phys.* **1971**, *54*, 1418-1419.
(2) Redfield, A. G.; Kunz, S. D.; Ralph, E. K. *J. Magn. Reson.* **1975**, *19*, 114-117.
(3) Redfield, A. G. *Methods Enzymol.* **1978**, *49*, 253-270 and references cited therein.
(4) Lindon, J. C.; Ferrige, A. G. *Prog. NMR Spectrosc.* **1980**, *14*, 27-66 and references cited therein.
(5) Hore, P. J. *J. Magn. Reson.* **1983**, *55*, 283-300 and references cited therein.
(6) Davies, S.; Bauer, C.; Barker, P.; Freeman, R. *J. Magn. Reson.* **1985**, *64*, 155-159 and references cited therein.
(7) Yao, C.; Simplaceanu, V.; Lin, A. K.-L. C.; Ho, C. *J. Magn. Reson.* **1986**, *66*, 43-57 and references cited therein.
(8) Allerhand, A.; Addleman, R. E.; Osman, D. *J. Am. Chem. Soc.* **1985**, *107*, 5809-5810.
(9) Allerhand, A.; Dohrenwend, M. *J. Am. Chem. Soc.* **1985**, *107*, 6684-6688.
(10) Allerhand, A.; Addleman, R. E.; Osman, D.; Dohrenwend, M. *J. Magn. Reson.* **1985**, *65*, 361-363.
(11) Maple, S. R.; Allerhand, A. *J. Magn. Reson.* **1986**, *66*, 168-171.
(12) Allerhand, A.; Bradley, C. H. *J. Magn. Reson.* **1986**, *67*, 173-176.
(13) Maple, S. R.; Allerhand, A. *J. Am. Chem. Soc.* **1987**, *109*, 56-61.
(14) Maple, S. R.; Allerhand, A. *J. Magn. Reson.* **1987**, *72*, 203-210.
(15) Bammel, B.; Evilia, R. F. *Anal Chem.* **1980**, *52*, 1999-2000.

0002-7863/87/1509-6609$01.50/0

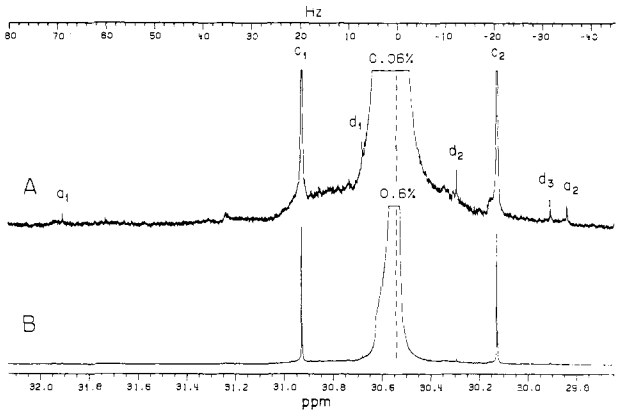

Figure 1. Region of the methyl resonance in the proton-decoupled ^{13}C NMR spectrum of **1** (with 20% v/v cyclohexane-d_{12}) recorded at 50.31 MHz and 26.5 °C, with 6000 scans. The main methyl carbon resonance is shown truncated (A) at 0.06% and (B) at 0.6% of its full peak height. For the upper scale, in Hertz, the main peak has been set to zero frequency. The lower scale is in parts per million downfield from Me_4Si. Other details are given in the Experimental Section. The $^1J_{CC}$ satellites which arise from $^{13}CH_3$–^{13}CO–$^{12}CH_3$, labeled c_1 and c_2, are truncated at about 10% of their full peak height in (A). The other labeled peaks are discussed in the text.

and Fourier transformation. The individual spectra were digitally shifted until the methyl carbon resonance of **1** was aligned in all 30 spectra, which were then added in the double-precision (40-bit word) mode. The absolute position of the main methyl resonance of **1** was not exactly the same in all 200-scan batches, because it exhibited a gradual downfield drift, as a result of a small change in solvent composition caused by different evaporation rates of **1** and cyclohexane-d_{12} (see section on Artifacts).

A spectrum of **1** from Fisher (with 20% v/v cyclohexane-d_{12}) was also recorded and processed essentially as described above, but with the use of 270° radio frequency pulse excitation[16,17] and only 3000 scans.

Rate of Aldol Condensation. One volume of 0.1 M sodium hydroxide was added to 20 volumes of a 4:1 (v/v) mixture of **1** and cyclohexane-d_{12}. Spectral accumulation was started immediately after addition of NaOH, with the use of 270° radio frequency pulse excitation,[16,17] a spectral width of ±300.12 Hz (quadrature detection), 64K time-domain points, an acquisition time of 54.59 s per scan, a 0.1-s interval between successive scans, and 4 scans per spectrum, which yielded an accumulation time of 3.64 min per spectrum. Twenty seven spectra were acquired, at times ranging from 25.5 to 9520 min after addition of NaOH. Each time-domain spectrum was subjected to 30-mHz digital Lorentzian broadening and Fourier transformation. Representative spectra are shown in Figure 2. The time dependence of the molarities of **1** and **2** was obtained from the spectra as described below.

Quantitative Analysis. Each integrated intensity was taken to be proportional to the product of the peak height and line width at half-height, a valid relationship for Lorentzian line shapes. The peak height and line width of each peak were obtained from the best fit of all digital data points above half-height (plus one more just below half-height on each side of the peak) to a Lorentzian curve. Each integrated intensity was then divided by its nuclear Overhauser enhancement (NOE) factor, defined here as the *ratio of intensities* with and without proton decoupling. The NOE measurement was done on the sample used for aldol condensation studies, 9150 min after addition of NaOH, when the equilibrium between **1** and **2** was fully established. NOE values were obtained from a comparison of integrated intensities in a fully proton-decoupled spectrum and one recorded with gated proton decoupling, set to remove the ^{13}C–^1H scalar splittings but without causing any Overhauser enhancement.[18] The spectral conditions for the fully proton-decoupled spectrum were the same as those for the kinetic study. For

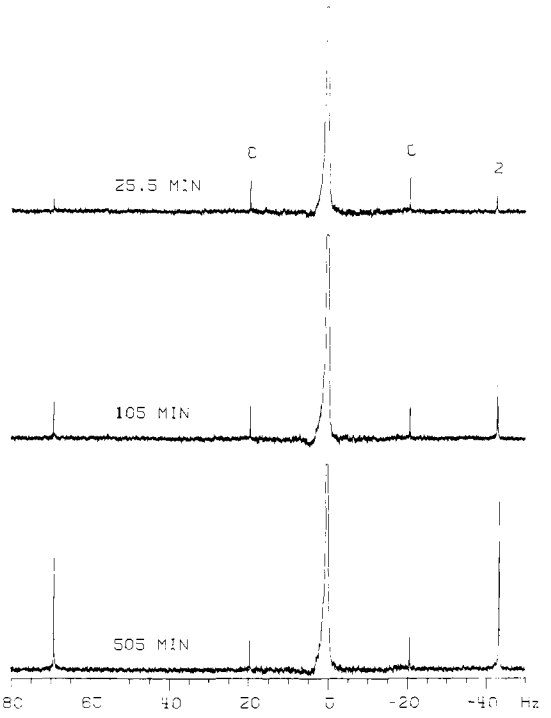

Figure 2. Region of the methyl resonance in proton-decoupled ^{13}C NMR spectra of **1** (with 20% v/v cyclohexane-d_{12}) recorded at 50.31 MHz and 26.5 °C, at various intervals (indicated on each spectrum) after addition of 5% v/v aqueous 0.1 M NaOH. Each spectrum is the result of 4 scans in a total accumulation time of 3.64 min. Other details are given in the Experimental Section. The peaks designated with C are the $^1J_{CC}$ satellites which arise from $^{13}CH_3$–^{13}CO–$^{12}CH_3$. Peaks 1 and 2 are the resonances of C-1 and C-5, respectively, of **2**.

the spectrum without Overhauser enhancement, the interval between the end of one scan and the beginning of the next one was increased from 0.1 s to 100 s, and the number of scans was increased from 4 to 16. The resulting NOE values were 2.0, 2.4, and 2.9 for the methyl carbon of **1**, C-1 of **2**, and C-5 of **2**, respectively. The molar ratio of **2** and **1** was taken to be the ratio of the integrated intensities of C-5 of **2** and the methyl carbon of **1**, divided by the corresponding ratio of NOE values. We established that, under our spectral conditions, differences in spin–lattice relaxation time (T_1) values did not affect the relative (and absolute) intensities of the methyl carbon resonances of **1** and **2**, as follows: (i) No intensity changes were detected when the recycle time (acquisition time per scan plus interval between successive scans) was increased from the 54.69 s of Figures 1 and 2 to 154.59 s, in measurements made on the same sample as for the NOE data. (ii) A T_1 measurement, done essentially as described,[9] yielded a value of 19.9 s for the methyl carbon of **1** of the sample of Figure 1.

The molar ratios of **1** and **2** obtained as described above, together with the initial concentration of **1** estimated as described below, yielded the time-dependent concentrations of both substances. The molarity of **1** at $t = 0$ was estimated with the use of the density of pure **1** by neglecting any volume changes caused by the addition of 20% v/v cyclohexane-d_{12} and the subsequent addition of 5% v/v of 0.1 M NaOH to the mixture of **1** and cyclohexane-d_{12}. The resulting estimated value is 10.3 M.

Chemical Shifts. Chemical shifts are presented either in hertz relative to the methyl carbon resonance of $^{13}CH_3$–^{12}CO–$^{12}CH_3$ or in parts per million from internal Me_4Si. However, the samples of Figures 1 and 2 did not contain Me_4Si. For these spectra, chemical shifts relative to Me_4Si were estimated indirectly from a spectrum of a sample of similar composition but with Me_4Si (see footnotes *a* and *c* of Table I). Chemical shifts were also determined for a sample of **2** (with 20% v/v cyclohexane-d_{12} and 1% v/v Me_4Si) that did not contain **1**. For both samples with Me_4Si, spectra were recorded with the use of 256K time-domain data points, a spectral width of ±6024 Hz (quadrature detection), a 10.88-s acquisition time per scan, and 0.1-Hz digital Lorentzian broadening. Chemical shift values were obtained by means of the same best-fit procedure described above for measurements of line widths and peak heights, except that only the 4 or 5 top points were used for the chemical shifts of the small peaks of Figure 1. The specific assignments for C-2, C-3, and C-4 of **2** (footnotes *b* and *c* of Table I) follow unambiguously from the large chemical shift differences and reported values for other compounds. However, our one-to-one assignments for C-1 and C-5 of

(16) We have established that the broad shoulder detectable on the downfield slope of a strong peak (see section on Artifacts) arises from regions of the sample of relatively low and inhomogeneous radio frequency field strength. A given flip angle for the main portion of the sample actually yields a range of shorter flip angles for the broad components. As a consequence, the relative intensities and phases of the narrow and broad components may be changed by using a nominal 270° instead of 90° flip angle, which may yield slight advantages in some cases. Details will be given elsewhere.[17]

(17) Maple, S. R.; Allerhand, A.; Bradley, C. H., in preparation.

(18) Freeman, R.; Hill, H. D. W.; Kaptein, R. *J. Magn. Reson.* **1972**, *7*, 327–329.

2 are based on the double intensity of the upfield methyl resonance relative to the downfield one.

Detection of Minor Components

Figure 1 shows the methyl carbon region in the ^{13}C NMR spectrum of **1** of natural isotopic composition (with 20% v/v cyclohexane-d_{12}), after 6000 scans with an acquisition time per scan of 54.59 s (which yields a digital resolution of 18.3 mHz), 30-mHz digital Lorentzian broadening in order to improve the signal-to-noise ratio, and no base line manipulation or other digital cosmetics. The major resonance, that of $^{13}CH_3$–^{12}CO–$^{12}CH_3$, is truncated at 0.06% (1/1667) and 0.6% (1/167) of its full peak height in Figure 1, spectra A and B, respectively.

The line width of the major resonance of Figure 1 is 77 mHz, which yields 47 mHz after subtraction of the 30-mHz digital broadening. We estimate a minimum natural line width contribution of 16 mHz, taken to be $(\pi T_1)^{-1}$. Therefore, the estimated maximum instrumental contribution is about 30 mHz, which includes about 10 mHz "extra" broadening from a non-optimum setting of the $(X^2 - Y^2)$ homogeneity correction gradient, set to reduce the amplitude of the downfield second-order spinning sideband.[17,19] Thus, no more than about 20-mHz instrumental broadening was feasible, even though the total accumulation time for the spectrum of Figure 1 was 108 h spread out over a 1-week period. Not only is the width at half-height very small, but the quality of the line shape down to 0.01% of full peak height and below permits unprecedented detection of very small peaks near a large one, as described below.

The methyl carbon region in the spectrum of **1** (Figure 1) contains two built-in sets of small resonances which have well-defined positions and intensities and which are therefore very suitable for calibrating the quality of resolution and accuracy of quantitation of minor components whose resonances are near those of major ones. We shall discuss these built-in calibrators prior to a discussion of the detection of **2**. The relatively large peaks at +19.455 and −20.849 Hz, labeled c_1 and c_2 and truncated at about 10% of their full peak height in Figure 1A, are the satellites which arise from the 1.1% (relative to $^{13}CH_3$–^{12}CO–$^{12}CH_3$) of $^{13}CH_3$–^{13}CO–$^{12}CH_3$ molecules as a result of ^{13}C–^{13}C scalar splitting,[20] with $^1J_{CC}$ = 40.30 Hz in this case. Each $^1J_{CC}$ satellite is expected to have 0.55% of the intensity of the main peak. The observed integrated intensities of peaks c_1 and c_2 are 0.55 and 0.54%, respectively.

The observation of $^1J_{CD}$ satellites, which arise from $^{13}CH_2D$–^{12}CO–$^{12}CH_3$ molecules in **1** of natural isotopic composition, is much more illustrative of the available resolution than the detection of $^1J_{CC}$ satellites, because the natural abundance of deuterium is only 0.015%. Three satellites of equal intensity are expected, because ^2H is a spin − 1 nucleus. However, each satellite should have an intensity of 0.015% (not 0.005%), because the threefold loss of intensity as a result of the $^1J_{CD}$ splitting is fully compensated by the threefold increase caused by equal probabilities of deuterium substitution at each of the three equivalent hydrogens. The following evidence indicates that peaks d_1, d_2, and d_3 (Figure 1A), at +7.03, −12.44, and −31.91 Hz, respectively, arise from $^{13}CH_2D$–^{12}CO–$^{12}CH_3$: (i) The integrated intensity of peak d_1 is difficult to measure, but those of peaks d_2 and d_3 are 0.014 and 0.012%, respectively, of the intensity of the main methyl carbon resonance; these values are, within experimental error, in agreement with the expected 0.015%. (ii) The observed peak separations yield $^1J_{CD}$ = 19.47 ± 0.01 Hz, in good agreement with the expected value of 19.45 Hz obtained from the measured $^1J_{CH}$ of 126.70 Hz multiplied by the ratio of the gyromagnetic ratios of ^1H and ^2H. (iii) The central component of the $^{13}CH_2D$–^{12}CO–$^{12}CH_3$ triplet (peak d_2) is 12.44 ± 0.01 Hz upfield of the resonance of $^{13}CH_3$–^{12}CO–$^{12}CH_3$, which yields a deuterium isotope effect on the ^{13}C chemical shift of 0.2473 ± 0.0002 ppm, consistent with a reported value of 0.250 ± 0.001 ppm for monodeuteriated acetone.[21]

We believe this is the first reported observation of $^1J_{CD}$ satellites in ^{13}C NMR spectra of samples of natural isotopic composition. Please note that peaks d_1 and d_2 are only about 7 and 12 Hz away from the major resonance and that their peak heights are actually only about 0.01% of the main peak height (less than the corresponding integrated intensity), because the $^1J_{CD}$ satellites have greater line widths (about 100 mHz in Figure 1A) than that of the main peak (77 mHz), probably as a result of a contribution from ^{13}C–^2H scalar relaxation.[22,23] Admittedly, most molecules are larger than acetone, and they will have line widths considerably greater than 77 mHz. However, we will show later in this paper that even when the line width of a major resonance is 0.5 Hz, it is still possible to resolve minor component (0.01%) peaks that are only 30 Hz away from the major one.

We assign peaks a_1 and a_2, at 68.82 and −35.31 Hz in Figure 1A, to C-1 and C-5 (a two-carbon resonance) of **2** on the basis of the following evidence: (i) After addition of 4% v/v **2** to **1** (with 20% v/v cyclohexane-d_{12} and 1% v/v Me_4Si) the resonances of C-1 and C-5 of **2** yield almost identical chemical shifts to those of peaks a_1 and a_2, respectively, of Figure 1A (Table I); the small discrepancies (less than 0.03 ppm) are attributable to the change in solvent composition when going from 4% **2** to just a trace of **2**. (ii) Upon addition of a small amount of aqueous NaOH to the sample of **1**, the intensities of peaks a_1 and a_2 increase with time (Figure 2 and Table I). (iii) The ratio of intensities of peaks a_1 and a_2 of Figure 1 is consistent with the corresponding value obtained from the spectrum of **2** dissolved in **1**.

The integrated intensities of peaks a_1 and a_2 (Figure 1A) are 0.004% and 0.014%, respectively, of that of the main resonance of **1**. When corrected for NOE differences (see Experimental Section) and the fact that a_1 is a single-carbon peak while a_2 and the methyl carbon resonance of **1** are two-carbon peaks, we get estimates of 0.007 and 0.01 mol % of **2** (relative to **1**) from a_1 and a_2, respectively, in the spectrum of **1** from Mallinckrodt (Figure 1). Peaks a_1 and a_2 in an analogous spectrum of "spectranalyzed" **1** from Fisher yielded 0.01 and 0.012 mol % of **2**, respectively. The above values correspond to a concentration of about 1 mM **2** in our acetone. This small amount is about 1/500 of the equilibrium concentration (see below), and it probably arises from the slow catalytic effect of trace impurities and/or the glass wall of the container.

Table I. Chemical Shifts (in Parts per Million from Me_4Si) of **2**[a]

solvent	[2]/M	carbon 1	carbon 5
2[b]	6.3	31.861	29.649
1[c]	0.3	31.912	29.810
1[d]	0.4	31.912[e]	29.673[f]
1[d]	0.04	31.917[g]	29.687[h]
1[i]	0.001	31.908[j]	29.838[k]

[a] For samples without Me_4Si, chemical shifts are referenced to the methyl carbon of **1**, taken to have a chemical shift of 30.540 ppm, the value obtained for the sample described in footnote *c*. [b] Sample of **2** with 20% v/v cyclohexane-d_{12} and 1% v/v Me_4Si. The chemical shifts of carbons 2, 3, and 4 were 209.409, 55.138, and 69.607 ppm, respectively. [c] About 76% v/v **1**, 4% v/v **2**, 19% v/v cyclohexane-d_{12}, and 1% v/v Me_4Si. The chemical shifts of carbons 2, 3, and 4 were 209.489, 55.409, and 69.639 ppm, respectively. [d] With about 20% v/v cyclohexane-d_{12}, 5% v/v H_2O, and 5 mM NaOH. [e] Peak 1 of the bottom spectrum of Figure 2. [f] Peak 2 of the bottom spectrum of Figure 2. [g] Peak 1 of the top spectrum of Figure 2. [h] Peak 2 of the top spectrum of Figure 2. [i] With 20% v/v cyclohexane-d_{12}. [j] Peak a_1 of Figure 1. [k] Peak a_2 of Figure 1.

(19) We have found that radio frequency inhomogeneity is the major contributor to spinning sidebands on our instrument. As a consequence, some shim settings which may minimize static magnetic field gradients do not yield minimum spinning sidebands. The $(X^2 - Y^2)$ shim setting which gives best static homogeneity yields considerably larger spinning sidebands than the value of $(X^2 - Y^2)$ which yields minimum sideband amplitudes. Details will be given elsewhere.[17]

(20) Wray, V. *Prog. NMR Spectrosc.* **1979**, *13*, 177–256.

(21) Arrowsmith, C. H.; Baltzer, L.; Kresge, A. J.; Powell, M. F.; Tang, Y. S. *J. Am. Chem. Soc.* **1986**, *108*, 1356–1357.

(22) Pople, J. A. *Mol. Phys.* **1958**, *1*, 168–174.

(23) Brevard, Ch.; Kintzinger, J. P.; Lehn, J. M. *Chem. Commun.* **1969**, 1193–1195.

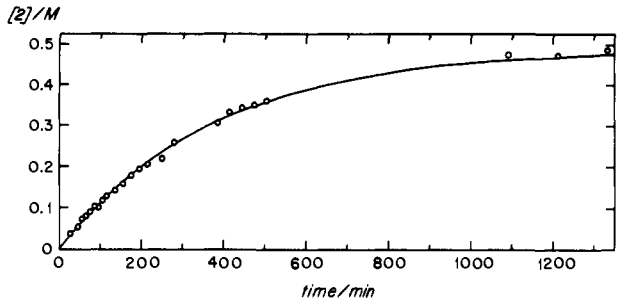

Figure 3. Time dependence of the molar concentration of **2** after addition of 5% v/v aqueous 0.1 M NaOH to **1** (which contained 20% v/v cyclohexane-d_{12}).

Rate of Aldol Condensation of Acetone

There are no reported *direct* measurements of the rate constant (k_2) for the aldol condensation of **1** into **2**, presumably because the equilibrium is highly displaced toward **1**, and therefore one has to measure the time dependence of small concentrations of **2** or very small changes in the large concentration of **1**. Values have been reported for the rate constant (k_1) of the dealdolization of **2** into **1**,[24-33] which together with the equilibrium constant $K = [\mathbf{2}]_e/[\mathbf{1}]_e^2$ can be used to calculate the value of k_2. Here $[\mathbf{1}]_e$ and $[\mathbf{2}]_e$ are the equilibrium molarities.

Figure 2 shows 3 out of 27 spectra of the methyl carbon region of **1** (with 20% v/v cyclohexane-d_{12}) recorded at various times (in the range 25.5–9520 min) after addition of 5% v/v aqueous 0.1 M NaOH. The truncated peak is the methyl carbon resonance of the $^{13}CH_3$–^{12}CO–$^{12}CH_3$ isotopomer of **1**, the peaks labeled with C are the $^{13}CH_3$–^{13}CO–$^{12}CH_3$ satellites, and peaks 1 and 2 are the resonances of C-1 and C-5, respectively, of **2** (labeled a_1 and a_2 in Figure 1). Integrated intensities corrected for NOE differences yielded the time dependence of [**2**], as described in the Experimental Section. The values of [**2**] up to $t = 1330$ min are shown in Figure 3. All 27 experimental points were fitted to the complete rate expression for the forward plus reverse reactions.

$$d[\mathbf{2}]/dt = k_2([\mathbf{1}]_0 - 2[\mathbf{2}])^2 - k_1[\mathbf{2}] \quad (1)$$

Here $[\mathbf{1}]_0$ is the initial concentration of **1**. We have assumed that $[\mathbf{2}]_0 = 0$, which neglects the 1 mM concentration of **2** already present in our sample of "pure" **1**. Substitution of k_1 by

$$k_1 = k_2([\mathbf{1}]_0 - 2[\mathbf{2}]_e)^2/[\mathbf{2}]_e \quad (2)$$

in eq 1 followed by integration and rearrangement yields

$$[\mathbf{2}] = [\mathbf{1}]_0^2[\mathbf{2}]_e(e^\alpha - 1)([\mathbf{1}]_0^2 e^\alpha - 4[\mathbf{2}]_e^2)^{-1} \quad (3)$$

where

$$\alpha = k_2 t([\mathbf{1}]_0^2 - 4[\mathbf{2}]_e^2)/[\mathbf{2}]_e \quad (4)$$

The value of $[\mathbf{2}]_e$ was determined from our spectra at large times after addition of NaOH. Equation 3 is essentially the standard one used for a reversible reaction which is second order in the forward direction and first order in the reverse direction,[34] adjusted for the specific stoichiometry of the aldol condensation of **1**. The curve shown in Figure 3 is the best fit of the 27 experimental values of [**2**] to eq 3, with k_2 and $[\mathbf{2}]_e$ as adjustable parameters, obtained by minimization of the sum of the square deviations, but with each square deviation weighted by $t^{1/2}$ in order to diminish the influence of [**2**] values near equilibrium. The best-fit values of k_2 and $[\mathbf{2}]_e$ are 1.2×10^{-5} M^{-1} min^{-1} and 0.49 M, respectively. The above value of $[\mathbf{2}]_e$ together with $[\mathbf{1}]_e = 9.3$ M yielded $K = 6 \times 10^{-3}$ M^{-1}, which then in conjunction with the above value of k_2 yielded $k_1 = 4.3 \times 10^{-3}$ min^{-1}. These values of K and k_1 are reasonably similar to reported ones obtained under different solvent conditions,[24,28] and in some reports different NaOH concentrations.[24,29]

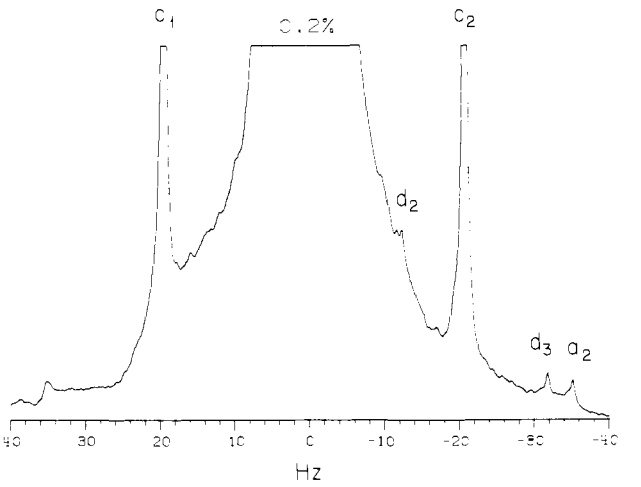

Figure 4. The ±40-Hz region of the spectrum of Figure 1, but processed with 0.4 Hz (instead of the 0.03 Hz of Figure 1) digital Lorentzian broadening. Peak designations are those of Figure 1. The main resonance of **1** is truncated at 0.2% of its full peak height.

Extension to Larger Molecules

The above results were obtained for a system which yielded natural line widths (W_0), defined here as the line widths at half-height in the absence of any instrumental contribution, of less than 0.1 Hz. Many kinetic and other types of studies of minor components will involve molecules much larger than **1** and **2**, which will yield more typical W_0 values of 0.5 Hz or more. In such cases, ultrahigh resolution spectra will yield observed line widths that are essentially equal to W_0.[9] Ultrahigh resolution methodology is still advantageous in such cases because it minimizes instrumental contributions on the skirts of the large peaks.[12-14] This is illustrated in Figure 4, which shows the ±40-Hz region of the spectrum of Figure 1, but processed with 0.4 Hz (instead of 30 mHz) digital Lorentzian broadening. Peaks d_3 and a_2 are still clearly resolved, even though their peak heights are about 1/7000 of that of the main resonance of **1**, and their positions are less than 40 Hz from the large peak.

When $W_0 = (\pi T_2)^{-1} = 0.5$ Hz and $T_1 = T_2$, then an acquisition time per scan of just a few seconds (instead of the 54.59 s used for Figure 1) is adequate and greatly reduces the total accumulation time per spectrum. In order to illustrate this point, Figure 4 was actually obtained from the first 6.8 s of the time-domain spectrum.

Artifacts

The observation of very small peaks in the presence of large ones places new demands on the NMR instrument, some of which are obvious, for example the need for adequate vertical digital resolution per scan (number of bits in the ADC) and in the accumulated signal (number of bits per address in data memory). Here we shall mention some less obvious instrumental requirements for the removal of imperfections. Two types of imperfections can interfere with ultrahigh resolution studies of minor components, some that affect the line shape of genuine peaks and others that create small spurious peaks that may be mistakenly taken for genuine minor component resonances. The hardware and software of commercial high resolution NMR instruments were not designed to take into account the requirements of ultrahigh resolution. Elimination of the artifacts mentioned below

(24) Koelichen, K. *Z. Phys. Chem.* **1900**, *33*, 129–177.
(25) Åkerlöf, G. *J. Am. Chem. Soc.* **1926**, *48*, 3046–3063.
(26) Åkerlöf, G. *J. Am. Chem. Soc.* **1927**, *49*, 2955–2981.
(27) Åkerlöf, G. *J. Am. Chem. Soc.* **1928**, *50*, 733–744.
(28) French, C. C. *J. Am. Chem. Soc.* **1929**, *51*, 3215–3225.
(29) Murphy, G. M. *J. Am. Chem. Soc.* **1931**, *53*, 977–981.
(30) Miller, J. G.; Kilpatrick, M., Jr. *J. Am. Chem. Soc.* **1931**, *53*, 3217–3224.
(31) La Mer, V. K.; Miller, M. L. *J. Am. Chem. Soc.* **1935**, *57*, 2674–2680.
(32) Westheimer, F. H.; Cohen, H. *J. Am. Chem. Soc.* **1938**, *60*, 90–94.
(33) Frost, A. A.; Pearson, R. G. *Kinetics and Mechanism*, 2nd ed.; Wiley: New York, 1961; Chapter 12, pp 335–350.
(34) See ref 33, Chapter 8, pp 186–187.

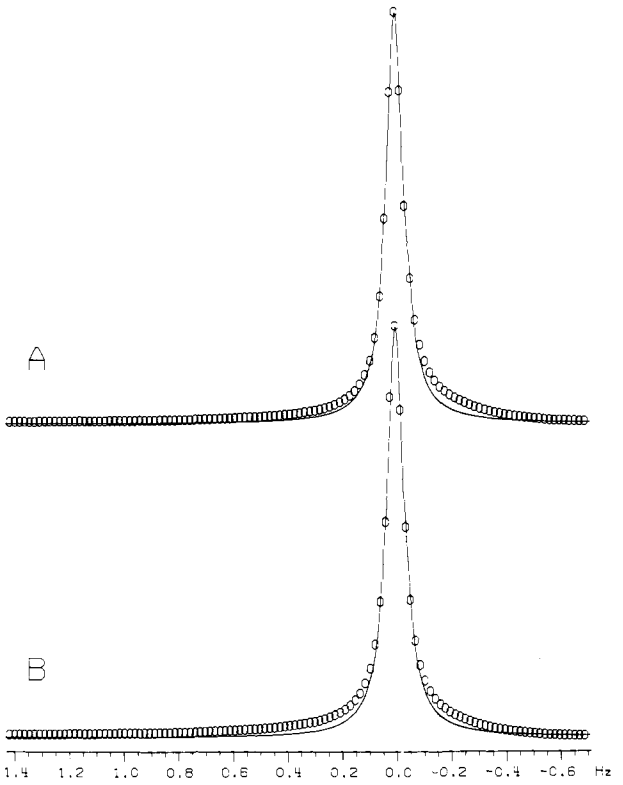

Figure 5. (A) The region from −0.71 to +1.43 Hz of the spectrum of Figure 1, but shown without truncation of the main resonance of **1**. The hexagons are experimental points and the curve is a best-fit Lorentzian. (B) Same as part A, but with the phase correction optimized for overall symmetry of the main peak.

will be facilitated by an understanding of their origin, which will require further investigations of various aspects of hardware and software.

Line Shape Artifacts. The dashed vertical line at zero frequency in Figure 1 runs through the center of the main resonance of **1**. Clearly, the line shape below 1% of full peak height is quite asymmetric, and it exhibits a "downfield" shoulder below about 0.3% of full peak height, which extends from about 2 to 8 Hz relative to the center frequency (Figure 1B). We have reason to believe that this shoulder arises from a small portion of the sample.[16] Elimination of this asymmetry by changes in probe design should improve the resolution of minor component peaks very close to the downfield edge of a major resonance.

One practical consequence of the above asymmetry occurs in the choice of phase correction. Figure 5A shows the region from +1.43 to −0.71 Hz of the main resonance of Figure 1. This region is exactly the truncated portion of Figure 1B. The hexagons are the experimental points and the curve is the best-fit Lorentzian. The phase correction of Figure 5A is that of Figure 1, which gives the best line shape symmetry below 0.06% of full peak height (Figure 1A), and is therefore a good choice for minor component detection, but not the best choice for overall peak symmetry. The best phase correction for overall symmetry is shown in Figure 5B, which differs by only 2.6° from the phase correction of Figure 5A.

During the recording of the spectrum of Figure 1 we encountered a rather unexpected line shape artifact which caused significant broadening of only one peak. In Figure 1, the line width of the resonance of C-1 of **2** (peak a_1) is 83 mHz, which is almost identical with the 77 mHz line width of the main resonance of **1**, but C-5 of **2** (peak a_2) has a line width of 190 mHz. However, spectra recorded in much less time than required for Figure 1 yielded a narrower C-5 resonance. For example, a sample of **1** with 5% v/v **2** and 19% v/v cyclohexane-d_{12}, after a total accumulation time of 3.6 min, yielded a 120 mHz line width for C-5 of **2** but essentially the same line widths as in Figure 1 for **1** and C-1 of **2**. The following evidence indicates that the "extra" 60 mHz in the line width of C-5 of **2** in the spectrum of Figure 1 was the result of changes in relative peak positions with time, during the 1 week of signal accumulation. The 6000-scan spectrum of Figure 1 resulted from the addition of 30 200-scan frequency-domain batches, after "alignment" of the main methyl carbon resonance of **1** in all 30 spectra (see Experimental Section). An examination of the absolute position of the main methyl carbon resonance of **1** in each of the 30 200-scan batches revealed a monotonic downfield drift of about 0.13 Hz/week. Unfortunately, Peaks a_1 and a_2 were undetectable in a single 200-scan batch. Therefore, we added the first 7 batches together and, separately, the last 7 ones. We processed the resulting two 64K time-domain spectra with an additional 64K of "zero-fill" points, in order to improve the final digital resolution to 9.16 mHz. Chemical shifts, measured with a line shape fitting procedure, yielded downfield drifts of 0.13, 0.03, and 0.10 Hz for peak a_1, peak a_2, and the main methyl carbon of **1**, respectively. Therefore, the procedure we used to create the spectrum of Figure 1, which includes "alignment" of the main methyl carbon resonance of **1** in all 30 batches (see Experimental Section) should cause about 30 and 70 mHz broadening of peaks a_1 and a_2, respectively. We hypothesized that these effects were the result of slight chemical shift variations with changes in solvent composition, caused by different evaporation rates of **1** and cyclohexane-d_{12} from our sample tube, which was equipped with a perforated plastic cap designed to hold a "vortex preventer" firmly in place. Even though pure cyclohexane is less volatile than pure acetone, they form an azeotrope which contains 74.2 mol % of **1** at 25 °C.[35] The sample of Figure 1 contained about 85 mol % of **1**, which is in the range where the proportion of cyclohexane is greater in the vapor than in the liquid.[35] Therefore, evaporation should cause an increase in the proportion of acetone in our sample. We did a study of the relative chemical shifts of **1** and **2** as a function of slight deviations of the cyclohexane-d_{12} concentration. When going from a sample where the percentages (by volume) of **1**, **2**, and cyclohexane-d_{12} were 72.5, 4.5, and 23.0%, respectively, to one with 76.2, 4.8, and 19.0%, respectively, the absolute changes in the positions of peak a_1, peak a_2, and the main methyl carbon resonance of **1** were 1.14, 0.45, and 0.93 Hz downfield, respectively. The downfield moves of peaks a_1 and a_2 are about 1.2 and 0.5 times, respectively, of the move of the methyl carbon peak of **1**. The downfield drifts of peaks a_1 and a_2 of the sample of Figure 1 (see above) are about 1.3 and 0.3 times the drift of the main methyl carbon peak of **1**, but these values are crude estimates because of the limited signal-to-noise ratios of peaks a_1 and a_2 in the spectra used for drift determinations. We conclude that a small increase in the acetone/cyclohexane-d_{12} ratio fully explains the observed time-dependent behavior of the chemical shifts of the resonances of **1** and **2** during the data acquisition for Figure 1. Clearly, long-term signal averaging of ultrahigh resolution NMR spectra requires precautions against even the slightest changes in composition of the solvent.

Spurious Peaks. It is well-known that very large signal-to-noise ratios (for the large resonances), obviously required to observe minor component peaks without suppression of the major ones, may reveal a variety of spurious peaks that can interfere with the identification of minor components. Among such spurious peaks are spinning sidebands at $\pm n\nu_S$ relative to the main peak,[36] where ν_S is the spinning speed in hertz and n is a positive integer, cyclic sidebands caused by WALTZ-16 proton decoupling,[37,38] and spurious peaks caused by imperfect data accumulation and processing.[4,39-43]

(35) Puri, P. S.; Polak, J.; Ruether, J. A. *J. Chem. Eng. Data* **1974**, *19*, 87-89.
(36) Williams, G. A.; Gutowsky, H. S. *Phys. Rev.* **1956**, *104*, 278-283.
(37) Shaka, A. J.; Barker, P. B.; Bauer, C. J.; Freeman, R. *J. Magn. Reson.* **1986**, *67*, 396-401.
(38) Shaka, A. J.; Keeler, J. *Progr. NMR Spectrosc.* **1987**, *19*, 47-129.
(39) Cooper, J. W. *Comput. Chem.* **1976**, *1*, 55-60.
(40) Cooper, J. W. *J. Magn. Reson.* **1976**, *22*, 345-357.
(41) Cooper, J. W.; Mackay, I. S.; Pawle, G. B. *J. Magn. Reson.* **1977**, *28*, 405-415.
(42) Stejskal, E. O.; Schaefer, J. *J. Magn. Reson.* **1974**, *13*, 249-251.

In this study, the *integrated intensity* of spinning sidebands was minimized by careful magnet homogeneity adjustments,[17] and then the *height* of the sidebands was further diminished by modulation of ν_S,[15] in the range 10–20 Hz. The resulting spinning sidebands have a flat-top shape. The one at $+\nu_S$ is barely visible in Figure 1A as a base line rise in the 10–20 Hz range. It has a *height* of about 0.01% of the main peak, but it does not interfere with minor component detection at the 0.01% level because of the broad flat-topped shape.

Cyclic sidebands caused by WALTZ-16 proton decoupling[37,38] were detected, outside the spectral range shown in Figure 1. They had a peak height less than 0.1% of that of the main resonance. Other spurious peaks occurred at frequencies related to that of the main resonance (ν_0), defined here as the difference between the resonance frequency and the phase detection carrier frequency, and the Nyquist frequency (ν_N), equal to half of the *full* spectral width when quadrature detection is used. We observed small ($\leq$0.03%) spurious peaks at $-\nu_0$, $\pm 2\nu_0$, and $\pm 3\nu_0$. In some spectra, we also detected very small ($\leq$0.01%) spurious peaks at $-(2\nu_N - 5\nu_0)$, $\pm(2\nu_N - 4\nu_0)$, and other positions. We are confident that a systematic study of these artifacts will yield procedures for reducing their levels even further.

Conclusions

Ultrahigh resolution methodology expands the range of applications of NMR to studies of minor components whose resonances are very close to those of major ones, even when the proportion of the minor component is 1/10000 of that of a major one. In this paper we have used ^{13}C NMR of samples of natural isotopic composition, a low-sensitivity technique. Each spectrum of Figure 2 required less than 4 min signal averaging time, because the proportion of the minor component (**2**) was $\geq$0.4% of that of the major one (**1**), but about 1 week of instrument time was used to observe 0.01% of **2** (Figure 1). However, detection of minor components at the 0.01% level by natural-abundance ^{13}C NMR can be achieved with just overnight data accumulation if the molecules are much larger than **1** and **2**, so that they have T_1 values shorter than 1 s[44] instead of the 20 s T_1 of **1**, because then the acquisition time per scan can be diminished from the 55 s used in this paper to 5 s or less. The resulting loss in digital resolution is not a problem because $W_0 > 0.32$ Hz when $T_2 < 1$ s. Furthermore, the signal-to-noise ratio per scan can be greatly increased by going from our low magnetic field (50-MHz ^{13}C and 200-MHz ^1H resonance frequencies) to high-field instruments (125-MHz ^{13}C and 500-MHz ^1H resonance frequencies), which should yield the signal-to-noise ratio of Figure 1 with the use of overnight signal accumulation. Finally, ultrahigh resolution methodology is not restricted to ^{13}C NMR. The conclusions of this report can be extrapolated to the more sensitive ^1H, ^{19}F, and ^{31}P NMR techniques.

Acknowledgment. This work was supported by grants from the National Science Foundation (PCM 83-04699) and the National Institutes of Health (GM 22620). We thank Robert E. Addleman and Deon Osman for their help in many ways.

(43) Stejskal, E. O.; Schaefer, J. *J. Magn. Reson.* **1974**, *14*, 160–169.

(44) Allerhand, A.; Doddrell, D.; Komoroski, R. *J. Chem. Phys.* **1971**, *55*, 189–198.

Heterogeneous Fluorescence Decay of (4→6)- and (4→8)-Linked Dimers of (+)-Catechin and (−)-Epicatechin as a Result of Rotational Isomerism

Wolfgang R. Bergmann, Mary D. Barkley, Richard W. Hemingway, and Wayne L. Mattice*

Contribution from the Institute of Polymer Science, The University of Akron, Akron, Ohio 44325, Department of Chemistry, Louisiana State University, Baton Rouge, Louisiana 70803, and Southern Forest Experiment Station, Pineville, Louisiana 71360. *Received February 27, 1987*

Abstract: The time-resolved fluorescence of (+)-catechin and (−)-epicatechin decays as a single exponential. In contrast, dimers formed from (+)-catechin and (−)-epicatechin have more complex decays unless rotation about the interflavan bond is constrained by the introduction of a new ring. The fluorescence decay in unconstrained dimers is adequately described by the sum of two exponentials. In a peracetylated dimer, the relative preexponential factors are in excellent agreement with the relative populations of two rotational isomers deduced from high-resolution NMR spectra. Removal of the acetyl groups does not significantly change the ratio of the preexponential factors, but it yields a first-order NMR spectrum. The reduction in the energy barrier between the rotational isomers upon removal of the acetyl groups causes interconversion of the isomers to become fast on the NMR time scale. However, resolution of the two populations is maintained on the fluorescence time scale.

(+)-Catechin and (−)-epicatechin are the monomer units in a class of polymers, called condensed tannins or polymeric proanthrocyanidins, that are found in a wide variety of plants.[1-3] It is believed that these plant polymers act as defense mechanisms for plants.[4,5] They are thought to protect plants from herbivores by forming complexes with salivary proteins, giving rise to a highly astringent taste.[6-8] The polymeric proanthocyanidins also form indigestible complexes with the plant proteins, thereby limiting the nutritional value of the vegetation.[9] Condensed tannins are

* To whom correspondence should be addressed at The University of Akron.

(1) Haslam, E. *Phytochemistry* **1977**, *16*, 1625.
(2) Porter, L. J. *Rev. Latioam. Quim.* **1984**, *15(2)*, 43
(3) Hemingway, R. W. In *Natural Products Extraneous to the Lignocellulosic Cell Wall of Woody Plants*; Rowe, J. W., Ed.; Springer-Verlag: Berlin, in press; Chapter 6.6.
(4) Haslam, E. *Biochem. J.* **1974**, *139*, 285.
(5) Feeny, P. P. *Recent Adv. Phytochem.* **1976**, *10*, 1.
(6) Bate-Smith, E. C. *Food* **1954**, *23*, 124.

0002-7863/87/1509-6614$01.50/0